

The broad-band noise characteristics of selected anomalous X-ray pulsars and soft gamma-ray repeaters

B. Külebi¹*† and Ş. Balman^{1,2}*

¹*Department of Physics, Middle East Technical University, İnönü Bulvarı, 06531 Ankara, Turkey*

²*Astrophysics Missions Division, Research and Scientific Support Department of ESA, ESTEC, Postbus 299 SCI-SA, Keplerlaan 1, 2201 AZ Noorwijk ZH, The Netherlands*

Accepted 2009 March 2. Received 2009 March 2; in original form 2007 August 13

ABSTRACT

We present the broad-band noise structure of selected anomalous X-ray pulsars (AXPs) and soft gamma-ray repeaters (SGRs) in the 2–60 keV energy band. We have analysed *Rossini X-Ray Timing Explorer* Proportional Counter Array archival light curves for four AXPs and one SGR. We detect that the persistent emission of these sources shows band-limited noise at low frequencies in the range 0.005–0.05 Hz varying from 2.5 to 70 per cent integrated rms in times of prolonged quiescence and following outbursts. We discovered band-limited red noise in 1E 2259+586 only for ~ 2 yr after its major 2002 outburst. The system shows no broad-band noise otherwise. Although this rise in noise in 1E 2259+586 occurred following an outburst which included a rotational glitch, the other glitching AXPs showed no obvious change in broad-band noise, thus it does not seem that this noise is correlated with glitches. The only source that showed significant variation in broad-band noise was 1E 1048.1–5937, where the noise gradually rose for 1.95 yr at a rate of ~ 3.6 per cent per year. For this source the increases in broad-band noise was not correlated with the large increases in persistent and pulsed flux, or its two short SGR-like bursts. This rise in noise did commence after a long burst, however, given the sparsity of this event, and the possibility that similar bursts went unnoticed the trigger for the rise in noise in 1E 1048.1–5937 is not as clear as for 1E 2259+586. The other three sources indicate a persistent band-limited noise at low levels in comparison.

Key words: stars: coroneae – stars: neutron – stars: oscillations – X-rays: stars.

1 INTRODUCTION

Anomalous X-ray pulsars (AXPs) and soft gamma-ray repeaters (SGRs) are part of a new class of neutron stars (NSs), whose emission mechanisms commute with neither accreting X-ray pulsars nor radio pulsars (PSRs). Their periods are clustered between 2 and 12 s and they are characterized by their rapid spin-down ($\sim 10^{-13}$ – 10^{-11} s s⁻¹) and high quiescent luminosities ($\sim 10^{33}$ – 5×10^{35} erg s⁻¹) that can not be explained by spin-down mechanisms. They also show wide range of variability, including flux and pulse profile variations (Dib, Kaspi & Gavriil 2007; Tam et al. 2008), glitches (Dib, Kaspi & Gavriil 2008), bursts (Gavriil, Kaspi & Woods 2002) and strong timing noise (Baykal et al. 2000; Kaspi et al. 2001). Three SGRs are known to exhibit giant bursts (SGR 0526–66, SGR 1900+14, SGR 1806–20), in which two of these objects rapid quasi-periodic oscillations (QPOs) are detected

after the onset of their flares (SGR 1900+14, Strohmayer & Watts 2005; SGR 1806–20, Israel et al. 2005).

SGRs and AXPs are widely accepted as being magnetars, NSs with magnetic fields strengths greater than the quantum critical level (10^{14} – 10^{15} G), whose main source of energy is the dissipation of these fields (Duncan & Thompson 1992; Thompson & Duncan 1995). The magnetar model for these objects explains the SGR bursts and the large flares, and it predicted the AXP bursts which occurred in 1E 1048.1–5937 (Gavriil et al. 2002) and 1E 2259+586 (Gavriil & Kaspi 2002). Thompson & Duncan (1995) argue that the bursts are due to crustal cracking as a result of magnetic diffusion, and that the large flares are due to major reconfigurations of the global magnetic field (Thompson & Duncan 1995). Magnetar strength magnetic fields can also account for the rapid spin-down of these objects and the QPOs observed during large flares (e.g. Israel et al. 2005; Strohmayer & Watts 2005). The existence of a fossil disc, and accretion from it, has also been proposed to explain the persistent properties of these sources (van Paradijs, Taam & van den Heuvel 1995; Chatterjee, Hernquist & Narayan 2000; Alpar 2001). However, this model has difficulty explaining the giant flares, repeat bursts and the pulsed optical emission that exist in this class of objects.

*E-mail: bkulebi@astroa.physics.metu.edu.tr (BK); solen@astroa.physics.metu.edu.tr (ŞB)

†Present address: Astronomisches Rechen Institut, Mönchhofstr. 12-14, 69120 Heidelberg, Germany.

In this paper, we investigated the properties of the broad-band noise in selected AXPs and SGRs, and present plausible origins for it within the context of the above two models. For example, if AXPs and SGRs have fall-back discs that they accrete from, as has been suggested by Ertan et al. (2007), then we can compare this noise to that of other accreting sources. For instance, the broad-band noise in X-ray binaries spans a very broad range and is due to variable X-ray flux from the accretion disc. In corona hosting X-ray binaries, a contribution of the noise in the high frequency range is due to photon delays in Compton up-scattered radiation (van der Klis 2006 and references therein). This is important given that AXPs and SGRs show hard power-law-like tails in their energy spectra that are also most likely due to photons being up-scattered in energy. In the context of the magnetar model, these hard tails in AXPs and SGRs have been successfully modelled by resonant cyclotron scattering (Lyutikov & Gavriil 2006; Rea et al. 2008). We argue that resonant cyclotron scattering can also introduce broad-band noise in the frequency range observed for these sources. Thus, in order to discriminate between the two models it becomes of great interest to study the broad-band noise in AXPs and SGRs.

2 DATA AND OBSERVATIONS

To calculate the band-limited noise (BLN) of these objects we used the 2–60 keV archived public *Rossi X-Ray Timing Explorer* (*RXTE*) light curves. The *RXTE* archive has a total of 10 sources that are either AXPs or SGRs. We used only appropriate sets of data, eliminating sources depending on epochs, exposures, burst dates and objects in the field of view (FOV).

We recovered one known SGR and four known AXP observations with fields relatively free of other sources. The exceptions are 1E 1048.1–5937 with Eta Carinae and SGR 1806–20 with XTE J1810–197 in their FOV, which both do not effect the noise levels in our analysis. The variability of Eta Carinae occurs in a very different time-scale (~ 85 d; Corcoran et al. 1997) with respect to 256 s used in this study. XTE J1810–197 is a transient source which was quiescent during the observations in our analysis (Ibrahim et al. 2004). Other fields include strong and variable sources. The data were obtained by the Proportional Counter Array (PCA; Jahoda et al. 1996) instrument aboard *RXTE*. We obtained 125-ms resolution background subtracted light curves from archived standard products (StdProds) of *RXTE*. These light curves are screened through standard procedures; namely source elevation greater than 10° , pointing offset smaller than 0:02, also PCU turn-off times are subtracted through defining good time intervals. Backgrounds are generated by PCABACKEST command of FTOOLS with the use of background models of the relevant epoch. These net light curves also include the barycentrically corrected time columns, which were used in our analyses.¹ Only when necessary, particularly to check background effects, non-background subtracted light curves were created from original data using SEEXTRACT v4.2. The manipulation of the data was made with the FTOOLS v5.21 software.

In order to measure the broad-band noise, we derived and averaged several power spectra for each source. The power spectral densities (PSD) expressed were calculated in terms of the fractional rms amplitude squared following Miyamoto et al. (1991), and the expected white noise levels were subtracted hence leaving us with the rms fractional variability of the time series in units

of $(\text{rms}/\text{mean})^2/\text{Hz}$. We used in total 658 light curves for our analysis (151 for 1E 2259+586, 136 for 1E 1048.1–5937, 125 for SGR 1806–20, 82 for 1E 1841–045 and 153 for RXS J1708–40), each of which was segmented into 10–50 individual power spectra to construct average PSD in a given time line.

3 ANALYSIS AND RESULTS

In order to increase the signal-to-noise ratio of the PSD to look for broad-band noise, the averaged light curves are grouped in 3-month intervals yielding 20–50 ks long exposure times for each source. The burst intervals noted in Table 1 are excluded from our data samples to avoid additional red noise because of the light-curve variability during bursts. The remaining burst like features (especially for the bursting SGR 1806–20) and spurious events due to instrument errors are screened by hand from the light curves. We averaged several 256-s long PSD for each source.

Figs 1–4 show the representative averaged PSD fitted with a broken power-law model, $\gamma[1 + (x/\nu)^2]^{-\alpha}$, in which ν is the frequency, γ is the $(\text{rms}/\text{mean})^2/\text{Hz}$ value of the flat part, x is the cut-off

Table 1. Observation log of the light curves analysed in this work.

Object	Obs id	Ave. count rate (count s ⁻¹)	Burst ^a
1E 1048.1–5937	40083-08	3.889	No
1E 1048.1–5937	50082-04	3.771	No
1E 1048.1–5937	60069-03	3.302	Yes
1E 1048.1–5937	70094-02	7.030	No
1E 1048.1–5937	80098-02	5.667	No
1E 1048.1–5937	90076-02	3.580	Yes
1E 1048.1–5937	91070-02	3.255	No
1E 1048.1–5937	92006-02	3.457	No
1E 2259+586	20145-01	1.799	No
1E 2259+586	20146-01	2.269	No
1E 2259+586	40082-01	1.752	No
1E 2259+586	50082-01	1.167	No
1E 2259+586	60069-01	0.4600	No
1E 2259+586	70094-01	2.695	Yes
1E 2259+586	80098-01	1.765	No
1E 2259+586	90076-01	1.673	No
RXS J1708–40	40083-14	13.02	No
RXS J1708–40	50082-07	12.10	No
RXS J1708–40	60069-07	12.37	No
RXS J1708–40	60412-01	12.99	No
RXS J1708–40	70094-04	13.58	No
RXS J1708–40	80098-04	13.38	No
RXS J1708–40	90076-04	13.38	No
1E 1841–045	40083-11	9.521	No
1E 1841–045	50082-05	8.835	No
1E 1841–045	70094-03	9.937	No
1E 1841–045	90076-03	9.013	No
1E 1841–045	91070-03	9.006	No
SGR 1806–20	50142-01	7.626	Yes
SGR 1806–20	50142-03	7.607	Yes
SGR 1806–20	60121-01	7.053	Yes
SGR 1806–20	70136-02	10.69	Yes
SGR 1806–20	90073-02	10.93	Yes
SGR 1806–20	90074-02	12.70	Yes
SGR 1806–20	91062-02	8.721	Yes

^aObservation dates have been correlated with the GCN (http://gcn.gsfc.nasa.gov/gcn3_archive.html) burst data and relevant papers (see captions of Fig. 5).

¹ All of the procedures involved in order to produce StdProds are explained in http://heasarc.gsfc.nasa.gov/docs/xte/recipes/stdprod_guide.html

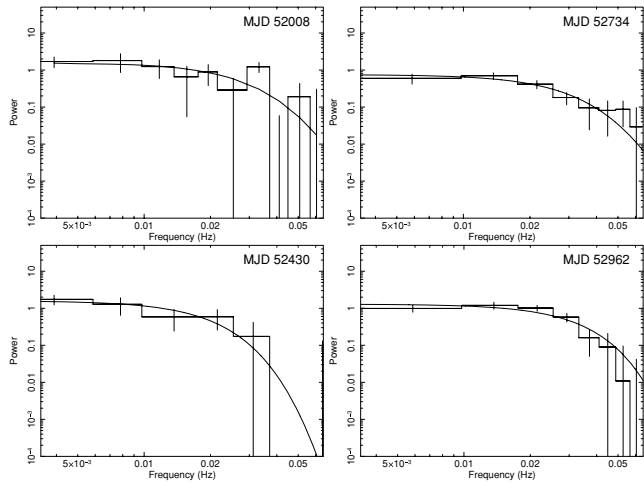


Figure 1. The averaged PSD in time showing the broad-band noise of AXP 1E 1048.1–5937. MJD 52211 and 52227 are burst epochs (Gavriil & Kaspi 2004). The time line increases top to bottom first, then from left to right.

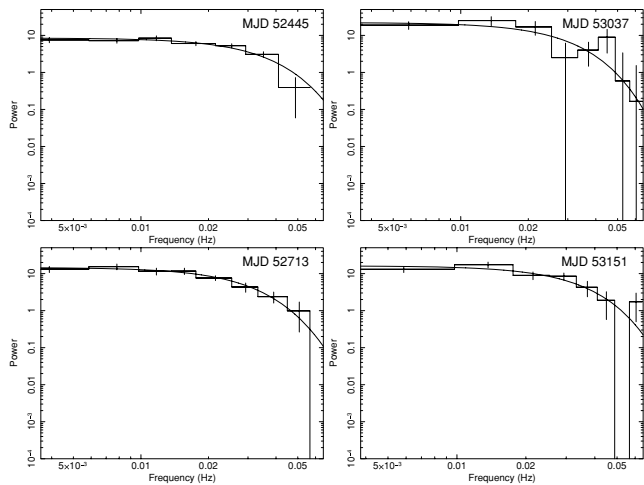


Figure 2. The averaged PSD in time showing the broad-band noise in AXP 1E 2259+586 with MJD 52443 as the burst epoch (Kaspi et al. 2003). The time line increases top to bottom first, then from left to right.

frequency and α is the power-law index. Each spectrum in the analyses is averaged over 3-month intervals and is separated by 5–900 d. In all sources, we find red noise with a break in the averaged PSD which may be considered BLN.

For all figures, the reduced chi-squares of the fits are between 0.6 and 1.2, the range of observed break frequencies are between 0.05 and 0.7 Hz and the power-law indices are between -0.5 and 375. Table 2 shows the list of power-law indices derived from the fits to PSD of the sources in time. An irregular variation of the indices in time is apparent. The ranges in Table 2 denote 1σ confidence level error ranges from fits. It is very hard to determine the value of these indices, since the decline in the power spectrum is near the edge of the sampling window and errors also increase considerably. We would like to make a note that for 2σ errors on the power-law index, the canonical value of -2 is in the acceptable range. In addition, the fitted PSD are integrated over 5×10^{-3} – 5×10^{-2} Hz interval to get the integrated fractional rms values. Time evolution of these values for 1E 1048.1–5937 and 1E 2259+586 are plotted in Fig. 5.

We found that for 1E 1048.1–5937 and 1E 2259+586 (two AXPs), their burst (maybe also flare) epoch correlate with their

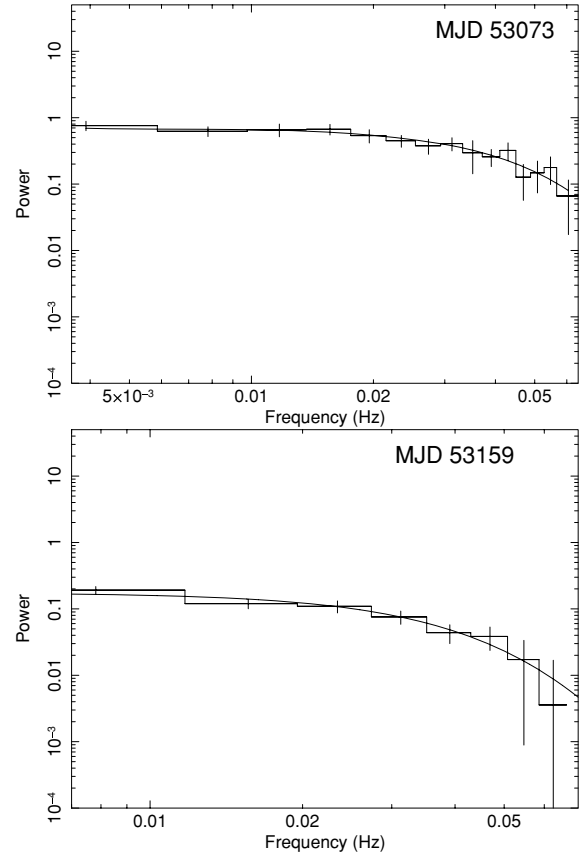


Figure 3. The averaged PSD in time showing the broad-band noise of 1E 1841–045 (top) and RXS J1708–40 (bottom).

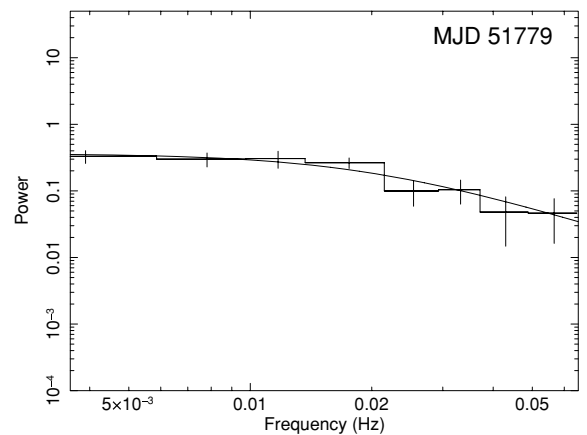


Figure 4. The time averaged PSD of SGR 1806–20 showing the broad-band noise.

broad-band noise levels. The steady ~ 15 per cent rms noise of 1E 1048.1–5937 showed a slight drop, during which two of its SGR-like short bursts and a flare appeared, to levels around ~ 10 per cent rms in 16 months. This low noise recovered throughout the next 5 months until it reached its former noise level (see Figs 1 and 5). The red noise level of the source rose after a long burst and later a glitch and large scale flux increase (Dib et al. 2007c; Tam et al. 2008) to levels ~ 25 per cent rms and stayed at this level (with some variability) for about 1.95 yr (see Fig. 5, top panel). 1E 2259+586 showed a slightly different behaviour. It had no detectable broad-band red noise in quiescence and developed

Table 2. The power-law indices of AXPs and SGRs derived from fitted PSD in this work.

Epoch (MJD)	Epoch range (d)	Index(–)	Index error
1E 1048.1–5937			
51321	±87	121.97	±43.73
52058	±50	9.99	±5.31
52160	±46	51.64	±25.73
52275	±42	32.16	±10.01
52478	±48	79.31	±18.1
52626	±42	279.25	±64.75
52777	±43	9.24	±2.39
53010	±48	191.55	±45.75
1E 2259+586			
52490	±45	29.07	±4.5
52601	±53	4.77	±2.17
52757	±44	90.01	±38.79
52863	±50	17.94	±3.35
52975	±47	256.15	±65.75
53087	±50	64.87	±27.39
53192	±41	144.65	±34.05
SGR 1806–20			
51693	±76	0.46	±0.08
51825	±46	0.98	±0.2
52065	±44	16.65	±6.41
53288	±43	1.72	±0.19
53148	±52	108.47	±9.74
53498	±48	32.11	±4.32
1E 1841–045			
51334	±74	18.37	±5.29
51534	±63	6.32	±2.06
51788	±60	24.13	±9.54
51931	±46	78.41	±38.69
52415	±66	30.36	±5.78
52598	±69	30.79	±7.52
52803	±77	124.95	±33.76
52940	±40	45.38	±10.03
53125	±52	39.15	±9.16
53486	±46	211.9	±57.5
53590	±44	13.37	±2.47
1RXS J1708–40			
51317	±102	46.69	±16.39
51530	±84	335.05	±179.05
51845	±190	371.07	±282.24
52044	±9	9.26	±4.74
52409	±43	0.63	±0.14
52538	±51	46.23	±11.45
52681	±37	375.75	±172.65
52794	±49	26.86	±8.55
52906	±47	160.75	±30.15
53009	±49	66	±26.16
53119	±35	24.87	±6.61
53206	±47	9.83	±2.04
53291	±34	53.45	±14.31

broad-band red noise around ~60 per cent rms level right after its burst active state and the on-set of a glitch, stayed consistently at this level throughout nearly 2 yr, until it diminished in about 1.5 months (at MJD 53233) (see Figs 2 and 5, bottom panel) back to its original level of no broad-band noise.

The other two AXPs 1E 1841–045 and RXS J1708–40 maintain a persistent broad-band noise level compared with the two AXPs discussed in the above paragraph. Sources showed around ~11 and ~7 per cent rms level noise for 1E 1841–045 and RXS J1708–40, respectively (with slight increase in time). The total time-span of the detected broad-band noise for the two different epochs for RXS J1708–40 were 2.3 (51215–52053 MJD) and 2.6 yr (52366–53325 MJD). Furthermore, for 1E 1841–045 the time-spans for two separate time epochs analysed in this work were 2 (51977–51260 MJD) and 3.5 yr (53635–52349 MJD). 1E 1841–045 also stands out as the noisier of the two. SGR 1806–20 exhibited broad-band noise slightly fluctuating about a persistent level of ~10 per cent, overall. The time-span of our analysis in two epoch ranges were 1.4 (51600–52100 MJD) and 1.7 yr (53000–53600 MJD). We had difficulty relating the burst activity and the PSD for SGR 1806–20 due to the existence of excessive number of bursts.

4 DISCUSSION

Fig. 5 shows the comparative evolution of the band-limited red noise in 1E 1048.1–5937 and 1E 2259+586. The ordinate is the integrated rms BLN and the abscissa is the time in MJD. The error in time (x error) is the total time of the accumulated observation IDs for each data point. The y error is the 1σ error in the integrated rms values. 1E 2259+586 showed the highest level of noise and longest duration of change. 1E 1048.1–5937 is the only source that showed a drop of the noise level assuming level at start of MJDs is the steady normal level of noise. It was also the most noisy source after 1E 2259+586. A significant rise of the rms broad-band noise level in 1E 1048.1–5937 (like 1E 2259+586) after the long-burst epoch at 53185 MJD is detected for about 1.95 yr (may have lasted about 3 yr judging from telegrams; Rea et al. 2007).

On the basis of torque noise, 1E 2259+586 is very quiet (Baykal et al. 2000; Gavriil & Kaspi 2002), but after its outburst and a glitch, 1E 2259+586 experienced rapid spin-down over 60 d (Woods et al. 2004) and showed an excess in infrared radiation (Hulleman et al. 2001). In this period 1E 2259+586 displayed BLN lasting for a time-scale of 2 yr and no band-limited red noise otherwise. 1E 1048.1–5937 shows a highly variable torque noise such that, it can not be phase connected for long time intervals which is consistent with accreting sources (Baykal et al. 2000; Kaspi et al. 2001). In our work, this source showed band-limited red noise at all times. The substantial increase of the broad-band noise of 1E 1048.1–5937 in Fig. 5 (from 15 to about 25–30 per cent) occurred gradually after the long burst (>699 s) at 53185 MJD (Gavriil, Kaspi & Woods 2006). Following this, there has been a flux increase (outburst like) from 1E 1048.1–5937 reported along with a spin-up glitch at 54186 MJD (Dib et al. 2007c; Tam et al. 2008). The decrease of this rise of the soft X-ray flux was reported to be at 54265 MJD (Rea et al. 2007; Tam et al. 2008). These latest dates are at the edge of our curve for 1E 1048.1–5937 in Fig. 5 and are not included in our results. However, it is clear that it follows our peak of integrated rms values for the source. We note that the rise in broad-band noise started much earlier than the flux outburst right after the long burst at 53185 MJD (Gavriil et al. 2006). On the other hand, we caution that given the sparsity of this event, and the possibility that similar bursts went unnoticed, this start for the rise in noise is not as clear as in 1E 2259+586. We also note that this increase in red noise is not very correlated with a large increase in persistent and pulsed flux in the early stages until the outburst-like flux increase. Prior to its burst at 53185 MJD and the broad-band noise increase, there was a slight decrease of red noise during which two SGR-like short bursts

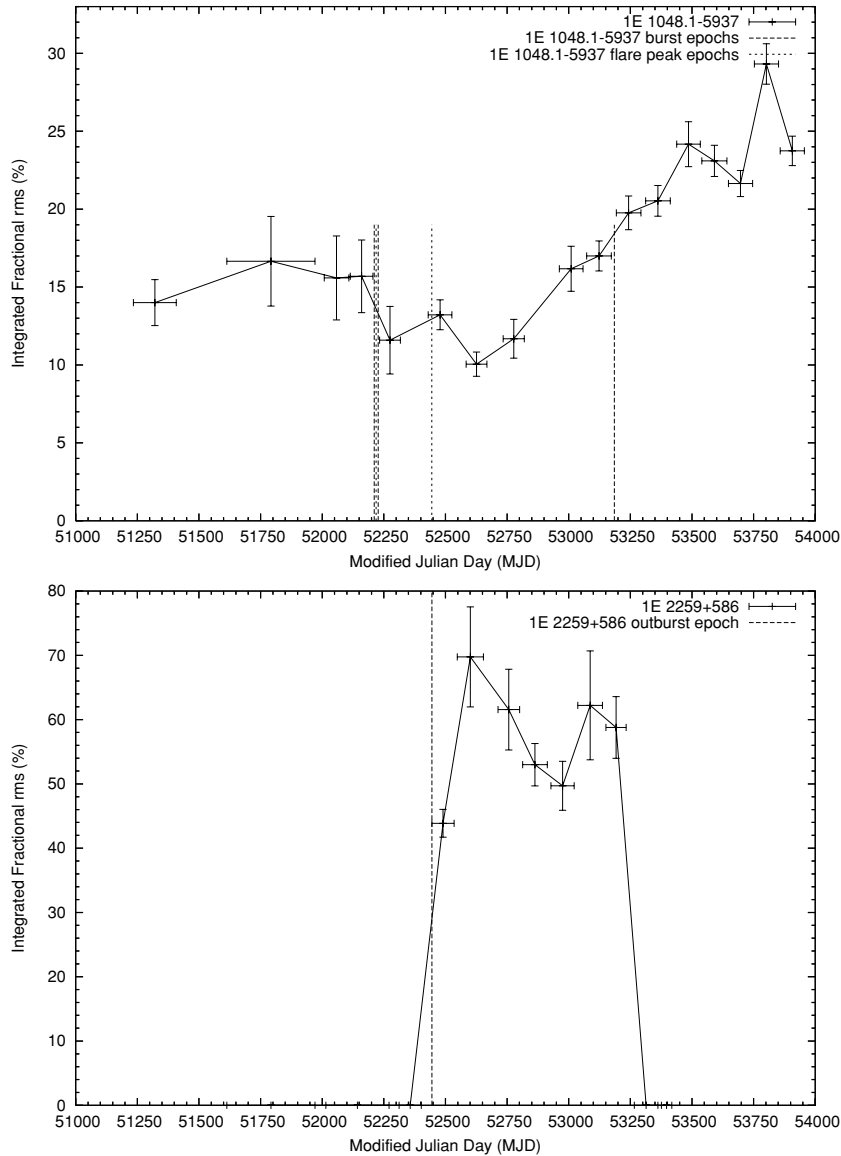


Figure 5. The integrated rms values for two AXPs (1E 2259+586 and 1E 1048.1–5937) in time. The model and the range of integration are described in the text. The burst epochs for 1E 1048.1–5937 are from Gavriil et al. (2002, 2006), flare epochs are from Gavriil & Kaspi (2004). The outburst epoch for 1E 2259+586 is from Kaspi, Gavriil & Woods (2002).

(52211 MJD and 52227 MJD) and two flares (52218 MJD and 52444 MJD) appeared (Gavriil et al. 2002; Gavriil & Kaspi 2004). The two bursts showed characteristics similar to SGR-bursts-like marginal pulsed flux increase not more than 3σ and short duration (<50 s first burst and <2 s second burst). Since we did not detect any correlation of broad-band noise with the SGR bursts in SGR 1806–20, we do not expect any effects here. The first flare starts between the two SGR-like bursts at 52218 MJD, after which an epoch of lower rms noise started. The drop of the broad-band noise showed a brief increase in the second flare (maximum at 52444.4 MJD, see Fig. 5) and the trend of decrease and recovery of noise after the flare is similar to the torque variability that was observed by Tam et al. (2008).

The time-averaged PSD of the four AXPs and the SGR showed in general very low frequency noise (VLFN). We detected that this noise to be band limited and in the frequencies higher than 0.05 Hz. There were little or no noise at all times below these frequencies

given the sensitivity of *RXTE* (also background) and statistical quality of *RXTE* light curves. The broad-band noise of AXPs and SGRs can be compared with the other isolated pulsars or X-ray binaries on the basis of their origin (e.g. accretion process, coronal activity, rotational variation). Broad-band noise in X-ray binaries is a result of a periodic X-ray flux variability in the form of continuum noise and QPOs with frequencies ranging from several mHz to more than thousand Hz (Hasinger & van der Klis 1989; van der Klis 2000, 2006). The flattening in the lower frequencies resemble PSD in disc-fed X-ray binaries, specifically the low hard state (LS) noise of black hole candidates and the VLFN of low magnetic field neutron star low-mass X-ray binaries (LMXBs; van der Klis 2006 and references therein). A flat topped noise arises in black hole candidates with large integrated rms noise level (~ 50 per cent) in the low frequencies (van der Klis 2006). The VLFN of LMXBs show the flat topped noise with a few per cent integrated rms and the continuum power-law component shows indices between -1.5 to

2, in general a range which holds for all the X-ray binaries (van der Klis 2006). The VLFN of the X-ray binaries is correlated with \dot{M} variations associated with an accretion disc and plausibly related to unsteady nuclear burning (van der Klis 2006). The structure of the flattening in the PSD sample of AXPs and SGRs resembles the VLFN of accreting X-ray binaries.

If one assumes that the variable X-ray flux originates from an accretion disc with a size between 1×10^9 and 1×10^{12} cm (values obtained from Ertan et al. 2007), the range of Keplerian frequencies ($r_K^3 = GM_{\text{NS}}/4\pi^2 v_K^2$) that should appear in the continuum noise is then from 0.058 to 2×10^{-6} Hz. This range overlaps with the detected range of broad-band noise in our work which supports that we could be detecting noise from the fall-back accretion discs suggested to exist in these systems (Ertan et al. 2007). However, the variations of this noise do not resemble the case for X-ray binary sources (see Fig. 5). In X-ray binaries outburst effects last for a few days to a week (where one detects a change in the broad-band noise level, as well). The persistent level of emission changes with accretion rate from high states to low states of X-ray binary sources while one also detects reallocation of broad-band noise from high frequencies into low frequencies. On the other hand, in our entire data set we did not detect any reallocation of noise, the noise we detected always appeared in the 0.05–0.005 Hz range and our time-scale for increased noise or high level of broad-band noise lasted for over a year or two which is not a detected phenomenon in X-ray binaries.

As discussed in the above paragraphs we favour that the changes in the band-limited low-frequency noise in magnetars are related most likely to the burst characteristics. Glitches seem to be the least effective of all in the broad-band noise changes from these sources. As discussed in the above paragraph, one origin for the detected broad-band noise in AXP and SGRs could be the suggested fall-back discs around these objects with the aforementioned caveats.

The origin of this noise could also be partially related to the frequency fluctuations of the NSs as in isolated pulsars and also to the variability that arises from the up-scattered radiation in their magnetospheres, particularly enhanced in the presence of a magnetar corona (Beloborodov & Thompson 2005, 2007). The plasma coronae in magnetars are a result of the starquakes and twisting of the magnetosphere that injects an electric current (i.e. plasma) into the stellar magnetosphere (Beloborodov & Thompson 2005, 2007). Emerging currents are maintained during the X-ray outburst and a dense thermalized plasma is present in the magnetosphere (lasting from 1 to 10 yr). Broad-band noise due to processes such as photon delays between soft and hard X-ray photons is well studied in X-ray binary sources, however, such time-scales are much shorter like a few milliseconds as a result of Compton up-scattering (in the presence of Thompson optical depth) from disc coronae (e.g. Schulz & Wijers 1993; Vaughan et al. 1994) which yields a continuum noise in very high frequencies in comparison with the frequency range we detect here (within 256 s). However, the processes in the magnetosphere of AXPs and SGRs are more complicated. Lyutikov & Gavril (2006) show that magnetospheric plasma can distort the thermal X-ray emission emerging from the star surface by repeated scatterings at the cyclotron resonance (e.g. resonant cyclotron scattering).

Recently, Rea et al. (2008) showed that an X-ray spectral model that involves resonant cyclotron scattering (together with a black-body model) successfully fits the soft X-ray emission (1–10 keV data) of 10 magnetars. If the dominant scattering process is the resonant scattering rather than Thompson scattering (as shown by Rea et al. 2008), then since the Thompson optical depth to scat-

tering is different than resonant scattering optical depth, the escape times of photons from the magnetosphere or an existing magnetar corona will be different in comparison with a simple disc corona where Thompson scattering optical depth dominates (as photons are Compton up-scattered in the corona). Once escape times differ, so will the time delays between soft and hard photons will be different in a resonant scattering dominated plasma. Rea et al. (2008) calculates the ratio of optical depths as $\tau_{\text{res}}/\tau_{\text{T}} = 10^5$ which strongly suggests that given similar geometries the high level of resonant optical depth to scattering should cause more delays in the emerging photons. If one assumes that scattering optical depth is directly proportional to number of scatterings, a millisecond delay then should become about 100 s delay, that could yield noise around 0.01 Hz. We suggest that especially for 1E 2259+586 this scattering can produce or contribute to the band-limited red noise we detect in the 0.005–0.05 Hz band and its changes. This is, also, supported by the commensurability of 2 yr rise in noise we detect in two AXPs and the magnetar coronal time-scale of 1–10 yr (time-scale the magnetar corona exists). Moreover, the increase in the photon indices of power-law tails in the X-ray spectra: for 1E 2259+586, Γ increases from -4.3 to -2.8 after the outburst (Woods et al. 2004; Kuiper et al. 2006); for 1E 1048.1–5937, Γ increases from -3.4 to -3.0 slowly after the reported burst at 53185 MJD and this increases to -2.3 after the flux outburst in 2007 March (Tiengo et al. 2005; Campana & Israel 2007; Rea et al. 2007; Tam et al. 2008).

Characteristic of the activity is important for inducing such a process e.g. a long burst or an outburst-like characteristic are necessary to produce such effects of highly increased broad-band noise levels. Glitches or flares show no effect or slight variations in noise levels. This supported by nearly stable BLN levels of 1RXS J1708–40 and 1E 1841–045 which show only glitches and no bursts.² Moreover, isolated pulsars that show glitches do not show such long-term significant rises in red noise levels in the low-frequency band.

Other models explaining the magnetar timing variabilities are ruled out mostly because of their time-scales. For example, seismic vibrations that are used to explain QPOs are very rapid and connected to giant bursts, and thus are not a satisfactory explanation for broad-band noise. One modifying principle for the seismic models is the propagation of Alfvén waves towards the core. Levin (2006) noted that these oscillations are a continuum, but they decay rapidly thus effectively they cannot correspond to our persistent rms noise observations.

5 CONCLUSIONS

We observed broad-band noise (BLN) in the four AXPs (1E 1048.1–5937, 1RXS 1708–40, 1E 1841–045 and 1E 2259+586) and an SGR (SGR 1806–20) mainly over the 0.005–0.05 Hz frequency band. The integrated rms values were in a range 2.5–15 per cent for four sources and 0 per cent rms for 1E 2259+586 before bursts. After bursts (our data do not include burst/outburst epochs) 20–70 per cent integrated rms noise was observed in two cases: 1E 2259+586 and 1E 1048.1–5937, respectively. The broad-band noise characteristics do not resemble either the accreting X-ray binaries or the isolated pulsars completely.

In general, we found that the four sources indicate a persistent level of integrated rms in time over a long base line of 3.5–5.5 yr which may be affected by noise from frequency fluctuations, and

² <http://www.physics.mcgill.ca/~pulsar/magnetar/main.html>

most likely as a result of variability due to resonant cyclotron scattering in a magnetar coronae and/or variability from existing fall-back discs around these objects. We also detected large-scale changes of the broad-band noise particularly due to long burst/outbursts. SGR-like bursts did not produce these type of variations in broad-band red noise, however, we believe that this is limited with the sensitivity of *RXTE* (also its background) and statistical quality of *RXTE* light curves. We calculate that 1E 2259+586 displays high level of broad-band noise lasting for a time-scale of 2 yr following its outburst and glitch. In addition, we observed significant rise of the rms broad-band noise level in 1E 1048.1–5937 for about 1.95 yr, after the burst epoch at 53185 MJD. We believe that this noise can relate to the existence of remnant discs suggested to exist around these objects, but the time-scale of changes after burst/outbursts are inconsistent with the observations in X-ray binaries. We stress that the changes in the broad-band noise levels are related to resonant cyclotron up-scattered radiation in AXP and SGR spectra. Correlation with long bursts and outbursts indicates an origin in the variability associated with the magnetar coronae. The typical time-scales of existence of magnetar coronae of 1–10 yr is consistent with the long-term variation of BLN detected in our work.

ACKNOWLEDGMENTS

We thank an anonymous referee for critical reading of the manuscript which improved this paper greatly. We also thank Altan Baykal and Ali Alpar for helpful comments. BK acknowledges support from TÜBİTAK, the Scientific and Technological Research Council of Turkey, through project 106T040. ŞB acknowledges an ESA fellowship and support from the Turkish Academy of Sciences with TUBA-GEBIP (Young Distinguished Scientist award) fellowship.

REFERENCES

- Alpar M. A., 2001, *ApJ*, 554, 1245
 Baykal A. S. T., Swank J., Alpar M. A., Stark M. J., 2000, *MNRAS*, 319, 205
 Beloborodov A. M., Thompson S., 2005, *ApJ*, 634, 565
 Beloborodov A. M., Thompson S., 2007, *ApJ*, 657, 967
 Campana S. M., Israel G. L., 2007, *Astron. Telegr.*, 1043
 Chatterjee P., Hernquist L., Narayan R., 2000, *ApJ*, 541, 367
 Corcoran M. F., Ishibashi K., Davidson K., Swank J. H., Petre R., Schmitt J. H. M. M., 1997, *Nat*, 390, 587
 Dib R., Kaspi V., Gavriil F., 2007, *ApJ*, 666, 1152
 Dib R., Kaspi V., Gavriil F., 2008, *ApJ*, 673, 1044
 Dib R., Kaspi V., Gavriil F., Woods P. M., 2007c, *Astron. Telegr.*, 1041
 Duncan R. C., Thompson C., 1992, *ApJ*, 392, L9
 Ertan Ü., Alpar M. A., Erkut M. H., Ekşi K. Y., Çalışkan Ş., 2007, *Ap&SS*, 308, 73
 Gavriil F. P., Kaspi V. M., 2002, *ApJ*, 567, 1067
 Gavriil F., Kaspi V. M., 2004, *ApJ*, 607, 959
 Gavriil F. P., Kaspi V. M., Woods P. M., 2002, *Nat*, 419, 142
 Gavriil F. P., Kaspi V. M., Woods P. M., 2006, *ApJ*, 641, 418
 Hasinger G., van der Klis M., 1989, *A&A*, 225, 79
 Hulleman F., Tennant A. F., van Kerkwijk M. H., Kulkarni S. R., Kouveliotou C., Patel S. K., 2001, *ApJ*, 563, L49
 Ibrahim A. I. et al., 2004, *ApJ*, 609, L21
 Israel G. L. et al., 2005, *ApJ*, 628, L53
 Jahoda K., Swank J. H., Giles A. B., Stark M. J., Strohmayer T., Zhang W., Morgan E. H., 1996, *Proc. SPIE*, 2808, 59
 Kaspi V. M., Gavriil F. P., Chakrabarty D., Lackey J. R., Muno M. P., 2001, *ApJ*, 558, 253
 Kaspi V. M., Gavriil F. P., Woods P. M., 2002, *Astron. Telegr.*, 99
 Kaspi V. M., Gavriil F. P., Woods P. M., Jensen J. B., Roberts M. S. E., Chakrabarty D., 2003, *ApJ*, 588, L93
 Kuiper L., Hermsen W., den Hartog P. R., Collmar W., 2006, *ApJ*, 645, 556
 Levin Y., 2006, *MNRAS*, 368, L35
 Lyutikov M., Gavriil F. P., 2006, *MNRAS*, 368, 690
 Miyamoto S., Kimura K., Kitamoto S., Dotani T., Ebisawa K., 1991, *ApJ*, 383, 784
 Rea N., Tiengo A., Israel G. N., Campana S., 2007, *Astron. Telegr.*, 1121
 Rea N., Zane S., Turolla R., Lyutikov M., Götz D., 2008, *ApJ*, 686, 1245
 Schulz N. S., Wijers R. A. M. J., 1993, *ApJ*, 273, 128
 Strohmayer T. E., Watts A. L., 2005, *ApJ*, 632, L111
 Tam C. R., Gavriil F. P., Dib R., Kaspi V. M., Woods P. M., Bassa C., 2008, *ApJ*, 677, 503
 Thompson C., Duncan R. C., 1995, *MNRAS*, 275, 225
 Tiengo A., Mereghetti S., Turolla R., Zane S., Rea N., Stella L., Israel G. L., 2005, *A&A*, 437, 997
 van der Klis M., 2000, *ARA&A*, 38, 717
 van der Klis M., 2006, in Lewin W. H. G., van der Klis M., eds, *Compact Stellar X-Ray Sources*. Cambridge Univ. Press, Cambridge, p. 39
 van Paradijs J., Taam R. E., van den Heuvel E. P. J., 1995, *A&A*, 299, L41
 Vaughan B., van der Klis M., Lewin W. H. G., Wijers R. A. M. J., van Paradijs J., Dotani T., 1994, *ApJ*, 421, 738
 Woods P. M. et al., 2004, *ApJ*, 605, 378

This paper has been typeset from a $\text{\TeX}/\text{\LaTeX}$ file prepared by the author.